COMBINING FEATURES EXTRACTED FROM IMAGERY AND LIDAR DATA FOR OBJECT-ORIENTED CLASSIFICATION OF FOREST AREAS

T. Hermosilla, J. Almonacid, A. Fernández-Sarría, L.A. Ruiz, J.A. Recio

Geo-Environmental Cartography and Remote Sensing Group.
Departamento de Ingeniería Cartográfica, Geodesia y Fotogrametría.
Universidad Politécnica de Valencia. Camino de Vera s/n, 46022 Valencia, Spain.
txohergo@topo.upv.es

KEY WORDS: Object-oriented classification; feature extraction; high-resolution imagery; lidar; land cover mapping.

ABSTRACT:

During the last several years, lidar has become a widely used technique for data collection from the earth surface and vegetation canopy being the large volume of high density lidar data the main drawback for its interpretation and analysis. In addition, parcel-based segmentation of high-resolution remotely sensed data can provide convenient and useful spatial and structural information. In this paper, a methodology for semi-automatic updating of forest land use/land cover geo-spatial databases, using high spatial resolution imagery and lidar data, is presented. High spatial resolution multispectral imagery and low density lidar data (0.5 points/m^2) has been employed. Cartographic limits from a cadastre geospatial database have been used in order to segment the territory and create analysis objects. The objects are characterized using a set of descriptive features: spectral, structural, shape and texture features computed from the multispectral image. These features are combined with 3D features derived from lidar data: density profiles based indices and statistics from point cloud, intensity values and normalized digital surface models. The lidar descriptive features proposed provide a more intuitive interpretation of the vegetation canopy structure than the raw data. The classification is performed using the decision trees technique combined with the boosting multi-classifier. Classification assessment is done by using ground truth data.

1. INTRODUCTION

Remote sensing techniques are widely employed tools in forest management applications. Satellite optical imagery (St-Onge and Cavayas, 1997; Bruniquel-Pinel and Gastellu-Etchegorry, 1998), Radar (Austin et al., 2003; Kimball et al., 2004) or Lidar data (Lefsky et al., 1999; Næsset 2002; Popescu et al., 2007) have been frequently employed to carry out these studies. Integration of different data source allows for a better earth surface description and facilitates classification processes. In order to improve these classifications, many authors have combined multispectral and lidar data in forest environments (Wallerman and Holmgren, 2007; Antonarakis et al., 2008; Ke et al., 2010), but also in agricultural (Bork and Su; 2007) and urban areas (Walter, 2005).

During the last several years, lidar has become a popular technique for data collection from the earth surface and its elements, both anthropogenic and natural, such as the vegetation canopy. However, the large volume of high density lidar data makes difficult its interpretation and analysis. Object-based analysis approaches can help to handle this limitation. Cartographical boundaries from cadastral or agricultural geospatial databases to segment the data can be used.

The objective of this study is to define a comprehensive set of object-based descriptive features based on lidar data to describe and classify mixed agricultural and forest environments. Lidar and image data are combined by means of a parcel-based approach, using cartographic limits derived form a land use/land cover geospatial database.

2. STUDY ZONE AND DATA

The study has been performed in A *Limia,* a local administrative area (*comarca*) of Galicia, in northern Spain. This rural area presents large areas of agricultural crops, forest and shrublands.

The images and lidar data employed were acquired from the *Spanish National Plan of Aerial Orthophotography* (PNOA). The images have a spatial resolution of 0.25 m/pixel and 4 spectral bands: red, green, blue and near infrared. The images of *A Limia* were acquired between May and July of 2007. Lidar data were collected in October of 2009 with a nominal point cloud density of 0.5 points/m^2.

Cartographic boundaries to define the final objects (plots) were obtained from the Spanish *Land Parcel Identification System* (SIGPAC), a geospatial database oriented to agriculture management. In this cartography, plots represent a continuous area of land within a parcel for a single agricultural use (Mirón, 2005). The total number of plots of the study area was 468,721.

Field samples were collected at the same time than the images, and have square shape with side sizes of 350 or 500 meters, depending of the area

3. METHODOLOGY

A general description of the steps followed in the parcel-based classification methodological approach is done in this section, with references to documents containing a more exhaustive explanation. The main steps followed are: image and data pre-processing, selection of training samples, descriptive feature

extraction from images and lidar data, classification and evaluation.

3.1 Pre-processing

High resolution images presented a high pre-processing degree: geometric rectification, panchromatic and multispectral fusion, mosaicking, and radiometric adjustments. Additionally, in order to facilitate the descriptive feature extraction process, images were resampled to 0.5 m/pixel using bilinear interpolation, since this spatial resolution was found adequate for this application.

To obtain the physical heights of the elements present on the terrain (trees, building, etc.) a digital terrain model (DTM) is required (Figure 1.c). The normalized point cloud is computed as the difference of the lidar point cloud (Figure 1.a) and the DTM. The normalized digital surface model (nDSM) (Figure 1.b) is computed by calculating the differences between the digital surface model (DSM) and the DTM.

DTM computation involves the use of algorithms to eliminate points belonging to any object above ground surface, such as vegetation or buildings. Although there are several methods, a complete fully integrated process is difficult to achieve (Baltsavias 1999). In this study, an iterative process to select minimum elevations has been used. A similar methodology was applied by Popescu et al., (2002) or Clark et al. (2004) and is based on selecting points of minimum elevation in a series of progressively smaller analysis windows. First, an initial DTM is computed with the selected points. Then, new minimum elevations are chosen by using smaller analysis windows. Then these points are compared with the initial DTM. These points are accepted if the height difference is lower than a predefined height threshold. A comprehensive description of the DTM algorithm employed can be found in Estornell et al. (2009).
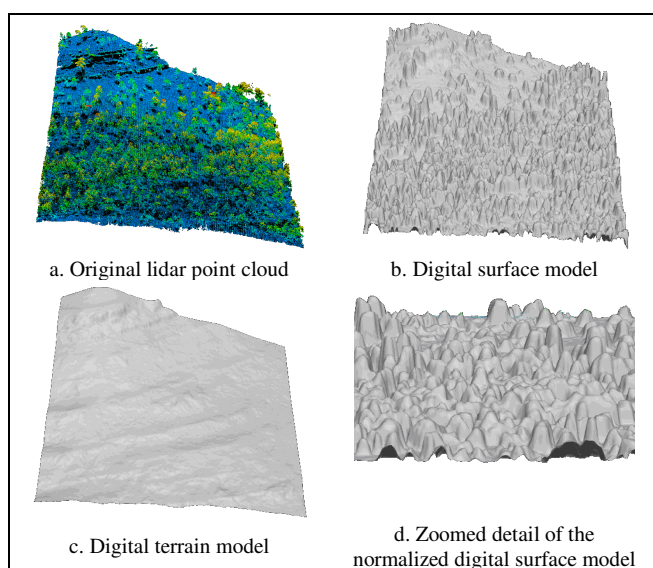
Spatial objects were created using the SIGPAC plot boundaries. Objects are described as contiguous pixel groups with similar characteristics to the real world elements that are modelling. To avoid the inclusion of pixels not belonging to the plot, due to errors in the delineation of limits or due to positional defects, a morphological erosion filtering was applied to each object with a circular structuring element of 5 pixels diameter. Besides, in order to confer coherence to the automatic feature extraction process, that requires a minimum object surface, plots with a surface lower than 60 m^2 were discarded.

Five generic classes were defined (see Figure 2): *Water layers, Buildings*, *Forest*, *Shrublands*, and *Arable and crop lands.* The class *Arable and crop lands* was subdivided in three subclasses for classifying in order to differentiate the vegetation level of the crop at the moment of the image acquisition: without, sparse and dense vegetation.

Most of training samples were selected from field databases. Since some sampling polygons did not coincide geometrically with the SIGPAC plots limits, the class assignation of samples was manually done. Additional samples were added by photointerpretation techniques in order to avoid the underrepresentation of some classes, especially *Water layers*, *Forest* and *Shrub lands*. As a result, a total of 1269 training samples were employed.

3.2 Feature extraction

Every plot was independently processed to extract descriptive features that characterize the current land use. Attending to he data source employed, the descriptive characteristics are divided in image and lidar features. Image features extracted in this study can be grouped in four categories: spectral, textural, structural and shape. Lidar features can be sub-divided attending to their nature as point cloud, nDSM, density profile, and intensity based.

a. Original lidar point cloud   b. Digital surface model

c. Digital terrain model   d. Zoomed detail of the normalized digital surface model

Figure 1. Models derived from lidar data.

a. Water   b. Building   c. Forest

d. Shrublands   e. Arable and crop lands (with and without vegetation)
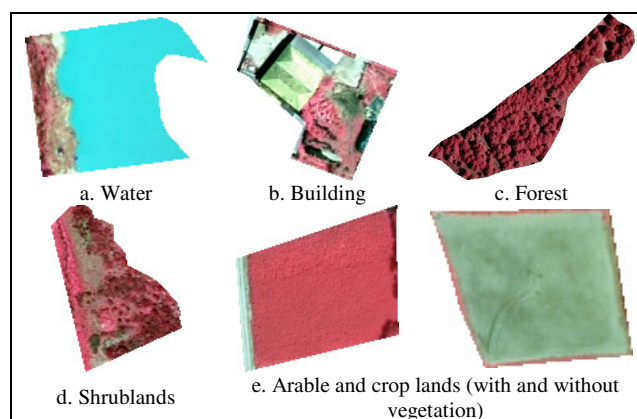
Figure 2. Examples of the classes defined in color infrared composition.

3.2.1 Image features

Spectral features provide information about the intensity values of objects on the visible and near infrared regions of the spectrum, which depends on land coverage types, state of vegetation, soil composition, construction materials, etc. These features are particularly useful in the characterization of spectrally homogeneous objects, such as herbaceous crops or fallow fields. Mean and standard deviation were computed from the bands NIR, R, G and also from the Normalized Difference Vegetation Index (NDVI).

Texture features inform about the spatial distribution of the intensity values in the image, being useful to quantify properties such as heterogeneity, contrast or uniformity related to each object (Ruiz et al., 2004). These properties are related to the land use/land cover inside an object. For each object a grey level co-occurence matrix (GLCM) characterizing the entire object was computed. From this matrix the features proposed by Haralick et al. (1973) were computed. Figure 3 shows some examples of GLCM computed for plots with different land uses. Texture information was completed with the values of kurtosis and skewness of the histogram, and the mean and the standard deviation of the edgeness factor for each plot (Sutton and Hall, 1972). The edgeness factor represents the density of edges present in a neighbourhood. Texture descriptive features were derived from the red band, since it was the band showing a better contrast.

Structural features describe the spatial arrangement of the objects in a plot. In this study, the structural features were extracted from the semivariogram graph computed for the NIR band. The semivariogram curve quantifies the spatial associations of the values of a variable, and measures the degree of spatial correlation between different pixels in an image. This is a particularly suitable tool in the characterization of regular patterns. For continuous variables the expression that describes the experimental semivariogram is:

$$(h) = \frac{1}{2N} \sum_{i=1}^{N} \left[z(x_i) - z(x_i + h) \right]^2$$

where $z(x_i)$ = value of the variable in position x_i.
   N = number of pairs of data considered.
   h = separation between elements in a given direction.

The experimental semivariogram representing each object is obtained by computing the mean of the semivariograms calculated in six directions, ranging from 0º to 150º with a step of 30º. Afterwards, each semivariogram curve is filtered using a Gaussian filter with a stencil of 3 positions, in order to smooth its shape and to eliminate experimental fluctuations. Some semivariogram graphs examples are shown in Figure 3, where this is noticeable that when a periodic spatial behaviour is produced, as in the citrus groves plot, the graph present a cyclic curve, known as *hole effec*t semivariogram (Pyrcz and Deutsch, 2003). Several structural descriptive features are computed considering the singular points of the semivariogram, such as the first maximum, the first minimum, the second maximum, etc., being described in detail in Balaguer et al. (2010).
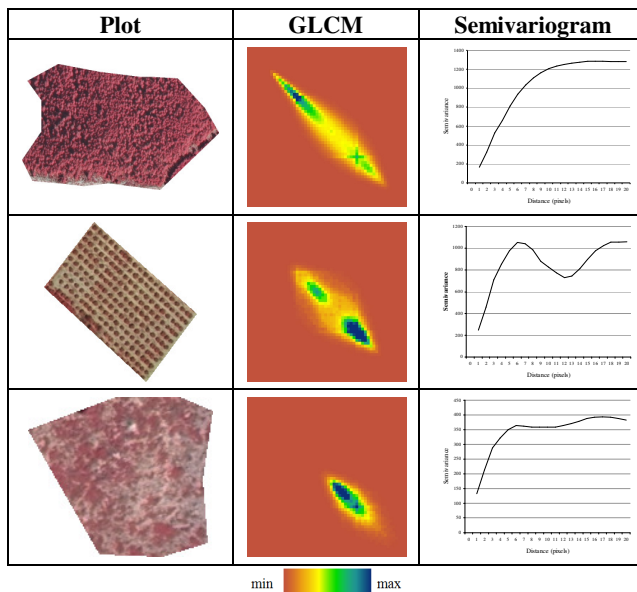
Figure 3. Graphic representation of grey level co-occurrence matrices (origin is in the top left corner) and semivariogram graphs computed *per-parcel* for different land uses: forest, citrus groves and shrublands.

Shape features inform about the complexity in the shape of the objects. They can contribute to differentiate polygons with specific shapes. Several standard features were extracted for each object: compactness, shape index, fractal dimension, area and perimeter.

3.2.2 Lidar features

Mean, standard deviation, maximum, skewness and kurtosis values have been computed for each plot from the normalized point cloud and from the nDSM (Figure 4). The descriptive features extracted from the nDSM provide information about the maximum height values, and their spatial distribution.

The features computed from the normalized point cloud show further information about the internal structure of the vegetation of a plot. In order to complement this internal information the percentiles 25, 50 and 75 were also computed. General statistics and percentiles from the intensity values of the point cloud have been extracted.
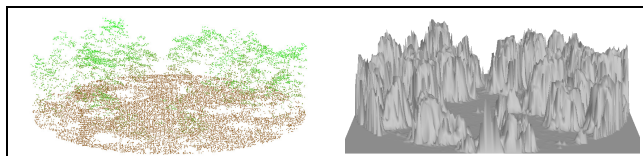
Figure 4. Normalized point cloud (left) and normalized digital surface model (right) example of a forest plot.

A deeper analysis of the normalized point cloud internal distribution structure can be done using the density profiles, which are the histograms of heights in each plot. Plots containing land uses, such as arable lands or irrigated crops (Figure 5c) present a very high percentage of points at the ground level, due to the absence of high vegetation (Figure 5d). Land uses characterized by the presence of dense vegetation,

like shrublands (Figure 5b), present more values above the ground level. When a plot is characterized by containing trees, like forest or citrus groves (Figure 5a), the density profile normally presents a peaks related with the height of clusters of diverse tree species or trees with different ages. This graph can be modelled by computing information regarding to the number of peaks, their position (height) and the percentage of points laying in that height.

a. Forest   b. Shrublands   c. Arable land
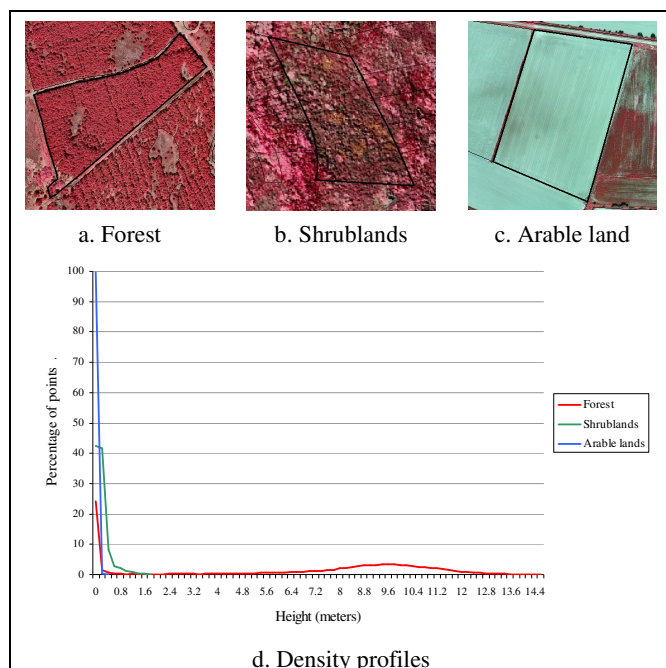
d. Density profiles

Figure 5. Density profiles for plots with different land uses: forest, shrublands and arable lands.

3.2.3 Feature selection

Due to the high number of features extracted from each object, some of them presented a high correlation, being redundant the information provided. The inclusion of these variables in the study could act as noise in the creation of the classification rules. The relations and redundancies existing between the descriptive features was initially analyzed by principal component analysis. Afterwards, linear descriptive discriminant analysis was applied in order to determine the significance of the features, removing from the study those with low significance level.

3.3 Classification through decision trees

Objects were classified by using decision trees. A decision tree is a set of organized conditions in a hierarchical structure, in such a way that the class assigned to an object can be determined following the conditions that are fulfilled from the tree roots (the initial data set) to any of its leaves (the assigned class). The algorithm employed in this study is the C5.0, which is the latest version of the algorithms ID3 and C4.5 developed by Quinlan (1993). This algorithm is the most widely used to deduce decision trees for classifying images (Zhang and Liu, 2005).

The process of building a decision tree begins by dividing the collection of training samples using mutually exclusive conditions. Each of these sample subgroups is iteratively divided until the newly generated subgroups are homogeneous, that is, all the elements in a subgroup belong to the same class. For each possible division of the initial data group, the impurity degree of the new subgroups is computed, and the condition which gives the lower impurity degree is chosen. This is iterated until the division of the original data into homogeneous subgroups is carried out by using the gain ratio as splitting criterion. This criterion employs information theory to estimate the size of the sub-trees for each possible attribute and selects the attribute with the largest expected information gain, that is, the attribute that will result in the smallest expected size of the sub-trees.

Objects were classified using 10 decision trees, by means of the boosting multi-classifier method, which allows for increasing the accuracy of the classifier. The methodology followed by the boosting to build the multi-classifier is based on the assignment of weights to training samples. The higher the weight of a sample, the higher its influence in the classifier. After each tree construction, the vector of weights is adjusted to show the model performance. In this way, samples which are erroneously classified increase their weights, whereas the weights of correctly classified samples decrease. Thus, the model obtained in the next iteration will give more relevance to the samples erroneously classified in the previous step (Hernandez-Orallo et al., 2004). After the construction of the decision tree set, the class to each object is assigned considering the estimated error made in the construction of each tree.

3.4 Evaluation

Cross validation technique was used to assess the classification of plots. From the confusion matrix (Aronoff, 1982; Congalton, 1991) the overall accuracy of the classification at plot level were computed. In addition the producer's and user's accuracies for each class, which respectively inform about the omission and commission errors, were calculated.

4. RESULTS

The results of the classification integrating image (spectral, texture, structural and shape) and lidar (intensity, nDSM, point cloud and density profiles) descriptive features are shown in Table 1. The results obtained improve the results that were attained in Hermosilla et al. (2010) using only image descriptive features (Table 2), where an overall accuracy of 91.4% was reached. The highest confusion was produced between the classes *Arable and crop lands* with *Shrublands*, and *Shrublands* with *Forest*. This confusion was produced due to the similarities between *Shrublands* and *Forest*, to the fuzzy border between both classes, and to the existence of mixed plots.

The addition of the lidar descriptive produces a increase of the overall accuracy up to 93.2 %. The producer's and user's accuracies of the different classes are generally improved. The most remarkable increments are the attained by the classes *Forest* and *Shrublands*.

		Reference					User's accuracy (%)
		Water	Buildings	Forest	Shrublands	Arable lands	
Classification	**Water**	16	1				94.1
	Buildings	1	174	2	3	3	95.1
	Forest		1	148	11	2	91.4
	Shrublands		5	12	262	20	87.6
	Arable lands	2	2		21	583	95.9
Producer's accuracy (%)		84.2	95.1	91.4	88.2	95.9	**93.2**

Table 1. Confusion matrix of the classification performed combining both image and lidar features.

		Reference					User's accuracy (%)
		Water	Buildings	Forest	Shrublands	Arable lands	
Classification	**Water**	17				2	89.5
	Buildings	1	175	3	5	4	93.1
	Forest			2	143	18	87.7
	Shrublands		3	14	251	28	84.8
	Arable lands	1	3	2	23	574	95.2
Producer's accuracy (%)		89.5	95.6	88.3	84.5	94.4	**91.4**

Table 2. Confusion matrix of the classification performed using image features.

Water Forest Arable lands
Buildings Shrublands
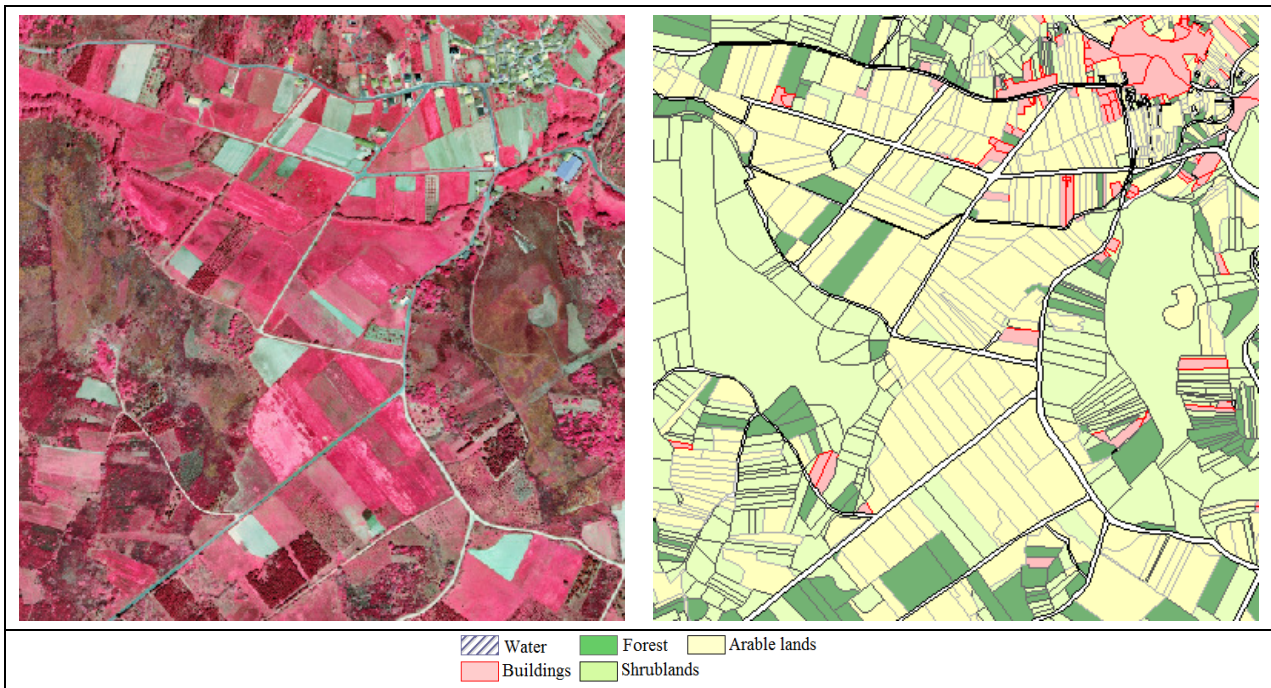
Figure 6. Colour infrared images (left) and land uses thematic map (right) obtained with the automatic classification.

5. CONCLUSIONS

This paper presents a methodology to combine imagery, cartography and lidar data to map forest areas. The proposed 3D features derived from lidar data complement the image-based features with non redundant information. A deeper analysis is necessary in order to determine the discriminant power of the features proposed.

The classification results show that integration of different data sources produce an improvement of the accuracies thanks to the better description of the objects.

ACKNOWLEDGEMENTS

REFERENCES

Antonarakis, A.S., Richards, K.S., Brasington, J., 2008. Object-based land cover classification using airborne LiDAR. *Remote Sensing of Environment*, 112(2008), pp. 2988–2998.

Aronoff, S., 1982. Classification accuracy: A user approach. *Photogrammetric Engineering & Remote Sensing*, 48(8), pp. 1299-1307.

Austin, J.M., Mackey, B.G., Kimberly, P.V.N., 2003. Estimating forest biomass using satellite radar: an exploratory

study in a temperate Australian Eucalyptus forest. *Forest Ecology and Management*, 176(1), pp. 575–583

Balaguer, A., Ruiz, L.A., Hermosilla, T., Recio, J.A., 2010. Definition of a comprehensive set of texture semivariogram features and their evaluation for object-oriented image classification. *Computers & Geosciences*, 36(2), pp. 231-240.

Baltsavias, E.P., 1999. Airborne laser scanning: existing systems and firms and other resources. *ISPRS Journal of Photogrammetry and Remote Sensing*, 66, pp. 164–198.

Bork, E.W., Su, J.G., 2007. Integrating LIDAR data and multispectral imagery for enhanced classification of rangeland vegetation: A meta analysis. *Remote Sensing of Environment*, 111(2007), pp. 11–24

Bruniquel-Pinel, V., Gastellu-Etchegorry, J.P., 1998. Sensitivity of texture of high resolution images of forest to biophysical and acquisition parameters. *Remote Sensing of Environment*, 65, pp. 61-85.

Clark, M.L., D.B. Clark, and D.A. Roberts, 2004. Small-footprint lidar estimation of sub-canopy elevation and tree height in a tropical rain forest landscape. *Remote Sensing of Environment*, 91, pp. 68-89.

Carr, J.R., 1996. Spectral and textural classification of single and multiple band digital images. Computers & Geosciences, 22(8), pp. 849-865.

Congalton, R., 1991. A review of assessing the accuracy of classications of remotely sensed data. *Remote Sensing of Environment*, 37(1), pp. 35-46.

Estornell, J., Ruiz, L.A., Hermosilla, T., 2009. Generación de un MDT a partir de datos Lidar utilizando procesos iterativos basados en la selección de alturas mínimas en una zona de montaña. *XIII Congreso Nacional de la Asociación Española de Teledetección*, 23-26 September 2009, Calatayud, Spain, pp.481-484.

Haralick, R.M., Shanmugam, K., Dinstein, I., 1973. Texture features for image classification. *IEEE Transactions on Systems, Man and Cybernetics,* 3(6), pp. 610-622.

Hermosilla, T., Díaz-Manso, J.M., Ruiz, L.A., Recio, J.A., Fernández-Sarría, A., Ferradáns-Nogueira, P., 2010. Parcel-based image classification as a decision-making supporting tool for the Land Bank of Galicia (Spain). *International Archives of the Photogrammetry, Remote Sensing and Spatial Information Sciences*, XXXVIII-4-8-2-W9, pp. 40-45.

Hernández Orallo, J., Ramírez Quintana, M.J., Ferri Ramírez, C., 2004. *Introducción a la minería de datos*. Pearson Educación S.A., Madrid.

Ke, Y., Quackenbush, L.J., Im, J., 2010. Synergistic use of QuickBird multispectral imagery and LIDAR data for object-based forest species classification. *Remote Sensing of Environment*, 114(2010), pp. 1141–1154.

Kimball, J.S., McDonald, K.C., Running, S.W., Frolking, S., 2004. Satellite radar remote sensing of seasonal growing seasons for boreal and subalpine evergreen forests. *Remote Sensing of Environment*, 90, pp. 243-258.

Lefsky, M., Cohen, W., Acker, S., Parker, G., Spies, T., Harding, D., 1999. Lidar remote sensing of the canopy structure and biophysical properties of Douglas-fir western hemlock forests. *Remote Sensing of Environment*,70, pp. 339–361.

Mirón, J., 2005. Cadastre and the reform of European Union's common agricultural policy. Implementation of the SIGPAC (1). *Catastro*, 54, pp. 161-172.

Næsset, E., 2002. Predicting forest stand characteristics with airborne scanning laser using a practical two-stage procedure and field data. *Remote Sensing of Environment*, 80, pp. 88–99.

Popescu, S.C., Wynne, R.H., Nelson, R.F., 2002. Estimating plot-level tree heights with lidar: local filtering with a canopy-height based variable window size. *Computers and Electronics in Agriculture*, 37, pp. 71-95.

Popescu, S.C., 2007. Estimating biomass of individual pine trees using airborne lidar. *Biomass & Bioenergy*, 31(9), pp.646-655.

Pyrcz, M. J., Deutsch, C. V., 2003. The whole story on the hole effect. In: Searston, S. (Eds.) *Geostatistical Association of Australasia Newsletter*, 18.

Quinlan, J.R., 1993. C4.5: *Programs for machine learning*. Morgan Kaufmann Publishing, San Francisco.

Ruiz, L.A, Fernández-Sarria, A., Recio, J.A., 2004. Texture feature extraction for classification of remote sensing data using wavelet decomposition: A comparative study. *International Archives of Photogrammetry, Remote Sensing and Spatial Information Sciences*, 35(B4), pp. 1109-1115.

Sutton, R.N., Hall, E.L., 1972. Texture measures for automatic classification of pulmonary disease. *IEEE Transactions on Computers*, 21(7), pp. 667-676.

St-Onge, B.A., Cavayas, F.,1997. Automated forest structure mapping from high resolution imagery based on directional semivariogram estimates. *Remote Sensing of Environment*, 61, pp. 82–95.

Wallerman, J., Holmgren, J., 2007. Estimating field-plot data of forest stands using airborne laser scanning and SPOT HRG data. *Remote Sensing of Environment*,110, pp. 501–508.

Walter, V., 2005. Object-based classification of integrated multispectral and Lidar data for change detection and quality control in urban areas. *International Archives of Photogrammetry, Remote Sensing and Spatial Information Sciences*, 36(8/W27), 6 p.

Zhang, S., Liu, X., 2005. Realization of Data Mining Model for Expert Classification Using Multi-Scale Spatial Data. International Archives of the Photogrammetry, *Remote Sensing and Spatial Information Sciences*, 26(4/W6), pp. 107-111.